

## Supplementary Information

### Photonic Si Microwell Architectures for Rapid Antifungal Susceptibility Determination of *Candida auris*

Christopher Heuer<sup>a,b,c</sup>, Xin Jiang<sup>a</sup>, Gali Ron,<sup>a</sup> Orna Ternyak<sup>d</sup>, Thomas Scheper<sup>b</sup>, Janina Bahnemann<sup>c</sup> and Ester Segal<sup>a\*</sup>

<sup>a</sup> Department of Biotechnology and Food Engineering, Technion – Israel Institute of Technology, 320003 Haifa, Israel, \*email: esegal@technion.ac.il

<sup>b</sup> Institute of Technical Chemistry, Leibniz University Hannover, 30167 Hannover, Germany

<sup>c</sup> Institute of Physics, University of Augsburg, 86159 Augsburg, Germany

<sup>d</sup> Micro- and NanoFabrication and Printing Unit, Technion – Israel Institute of Technology, Haifa, 3200003, Israel

### Experimental Procedures

**Materials, Media and Microbial Strains.** Glutaraldehyde, Roswell Park Memorial Institute medium (RPMI 1640), Cation-adjusted Muller Hinton broth (CAMHB), D-glucose, anidulafungin, amphotericin B and propidium iodide were supplied by Sigma-Aldrich, Israel. Absolute ethanol and all buffer salts (NaCl, KCl, KH<sub>2</sub>PO<sub>4</sub>, Na<sub>2</sub>HPO<sub>4</sub>.) and NaOH were purchased from Merck, Germany. 3-(N-morpholino)propanesulfonic acid (MOPS) was supplied by Chem-Impex International, Inc., USA. Potato Dextrose Agar (PDA) and Bacto agar were purchased from Difco, USA.

All aqueous solutions and media were prepared in Milli-Q water (18.2 MΩ cm). Phosphate buffered saline (PBS) was composed of 137 mM NaCl, 2.7 mM KCl, 1.8 mM KH<sub>2</sub>PO<sub>4</sub>, and 10 mM Na<sub>2</sub>HPO<sub>4</sub>. RPMI 1640 2 % G medium (RPMI 1640 medium supplemented with 2 % D-glucose; referred to as growth medium) was constituted of 10.4 g L<sup>-1</sup> RPMI 1640, 34.5 g L<sup>-1</sup> MOPS and 18 g L<sup>-1</sup> glucose, adjusted to pH 7.0 with 1 M NaOH and sterile filtered before use. PDA was prepared by suspending 39 g L<sup>-1</sup> PDA powder in water, followed by steam sterilization at 121 °C for 30 min before pouring the plates. CAMHB was prepared according to the manufacturer's instructions and supplemented with 15 g L<sup>-1</sup> Bacto agar for agar plate preparation. *Candida auris* (*C. auris*) DSM 21092 was obtained from the German Collection of Microorganisms and Cell Culture (DSMZ), Germany and *Saccharomyces cerevisiae* (*S. cerevisiae*) NCYC 1024 from the National Collection of Yeast Cultures, United Kingdom. *Escherichia coli* (*E. coli*) K12 was generously provided by Prof. Sima Yaron (Department of Biotechnology and Food Engineering – Technion)

**Preparation of Microbial Cultures.** All microbial cultures were stored at -80 °C. The yeasts *C. auris* and *S. cerevisiae* were refreshed on PDA and incubated for 16 - 18 h at 30 °C before cell suspensions in growth medium for antifungal susceptibility testing (AFST) experiments were directly prepared from these fresh agar plates. For iPRISM experiments, the cell suspension was adjusted corresponding to a turbidity standard of McFarland 2.0 (~10<sup>7</sup> cells ml<sup>-1</sup>), and for broth microdilution (BMD), cell suspensions with a cell density of ~10<sup>5</sup> cells mL<sup>-1</sup> were prepared. *E. coli* was refreshed on MHB agar plates and grown for 16 h at 37 °C. The bacterial cells were resuspended in MHB and adjusted to a cell density corresponding to a turbidity standard of McFarland 0.5 (~10<sup>8</sup> cells mL<sup>-1</sup>) before PRISM experiments were performed at 37 °C.

**Fabrication and preparation of photonic silicon chips.** Silicon chips with microwell gratings (dimensions: width of ~ 4 μm and depth of ~ 4 μm) were fabricated by laser writing and reactive ion etching techniques at the Micro- and Nano-Fabrication and Printing Unit (Technion) and cut into chips of 5 x 5 mm, as previously described.<sup>1</sup>

**(i)PRISM Assay.** A custom-made, aluminium flow cell was assembled as explained in our previous work<sup>2</sup> and controlled by a motorized linear stage (Thorlabs, Inc, USA) and LabView (National Instruments, USA) for incremental movement. Before each experiment, the system was rinsed with 70 % ethanol, and sterile water before growth medium was introduced to allow the medium, temperature (30 °C) and device to equilibrate. Afterwards, 500 μL of the yeast cell suspensions (McFarland 2.0) at varying antifungal concentrations were introduced while the zero-order reflected light was continuously recorded as follows. A 74-series collimating lens connected to a bifurcated fibre optic was arranged perpendicularly to the photonic silicon chips, illuminating them via an HL-2000 white light source, and the reflected light was recorded by a USB4000 CCD spectrometer (all Ocean Optics, USA). Fast Fourier transform (FFT) frequency analysis was performed on acquired reflectivity spectra in a

range between 450 to 900 nm, and the resulting single peak was identified by determining the maximum peak position, where the height of the detected peak directly corresponds to the intensity of the reflected light and the peak position to the  $2nL$  value ( $n$  = refractive index of the medium within the grating and  $L$  = depth of the microstructure). The intensity and  $2nL$  values were plotted versus time, and the per cent changes of the intensity  $\Delta I$  (%) and  $\Delta 2nL$  (%) were calculated as follows:

$$\Delta I (\%) = \frac{I - I_0}{I_0} \times 100 \% \quad \text{and} \quad \Delta 2nL (\%) = \frac{2nL - 2nL_0}{2nL_0} \times 100 \%$$

, where  $I_0$  and  $2nL_0$  refer to the values of  $2nL$  and intensity at  $t = 0$  min (introduction of cell suspensions). For AFST experiments,  $I_0$  and  $2nL_0$  were replaced by  $I_{90}$  and  $2nL_{90}$  ( $t = 90$  min) as occasionally the signals were unstable at the beginning of the assay, ascribed to the high number of introduced cells.

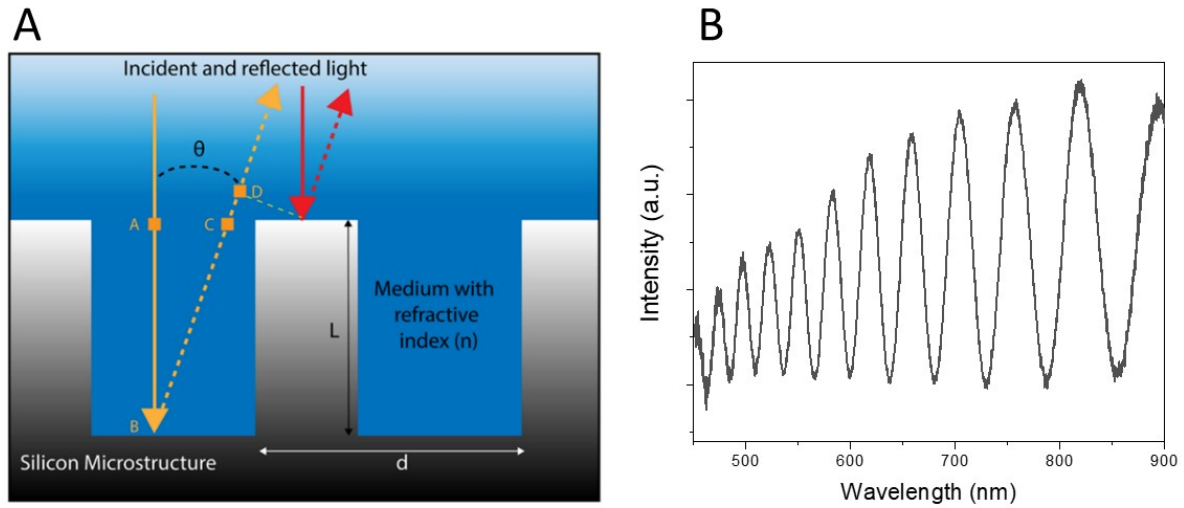
**Photonic Silicon Chips Characterization.** High-resolution scanning electron microscopy (HR-SEM) was performed using a Zeiss Ultra Plus high-resolution scanning microscope (Carl Zeiss, Germany). After sensing experiments, samples were fixated using 2.5 % glutaraldehyde in PBS and stored for at least 24 h at 7 °C. Subsequently, the chips were washed with water, dehydrated through a dilution series in ethanol (10 % - 50 % - 70 % - absolute ethanol) and gently dried under a stream of nitrogen before being observed using the scanning electron microscope.

Confocal laser scanning microscopy was performed using an LSM 700 confocal laser scanning microscope (Carl Zeiss, Germany) on samples where cells were stained with 20  $\mu\text{g mL}^{-1}$  propidium iodide after fixation in glutaraldehyde. The photoluminescence of the photonic silicon chips and fluorescence emitted by the propidium iodide-stained yeast cells were detected using 405 nm (Si photoluminescence) and 555 nm (propidium iodide) laser excitation wavelengths.

**Broth Microdilution AFST.** Broth microdilution (BMD) was performed based on the AFST protocol for yeasts of the European Committee for Antimicrobial Susceptibility Testing (EUCAST).<sup>3</sup> Briefly, two-fold dilution series of the antifungals anidulafungin and amphotericin B were prepared in growth medium and tested against a cell suspension (standardized cell density:  $10^5$  cells  $\text{mL}^{-1}$ ) of *C. auris* in a 96-well plate. Fungal growth was observed after incubation for 24 h at 30 °C by absorbance measurements (530 nm,  $n = 3$  for every tested concentration, Varioskan Flash, Thermo Scientific, USA). According to the EUCAST protocols, the MIC was defined as the lowest concentration of a drug that results in  $\geq 50$  % growth inhibition (anidulafungin) and  $\geq 90$  % growth inhibition (amphotericin B) compared to the untreated drug-free control.

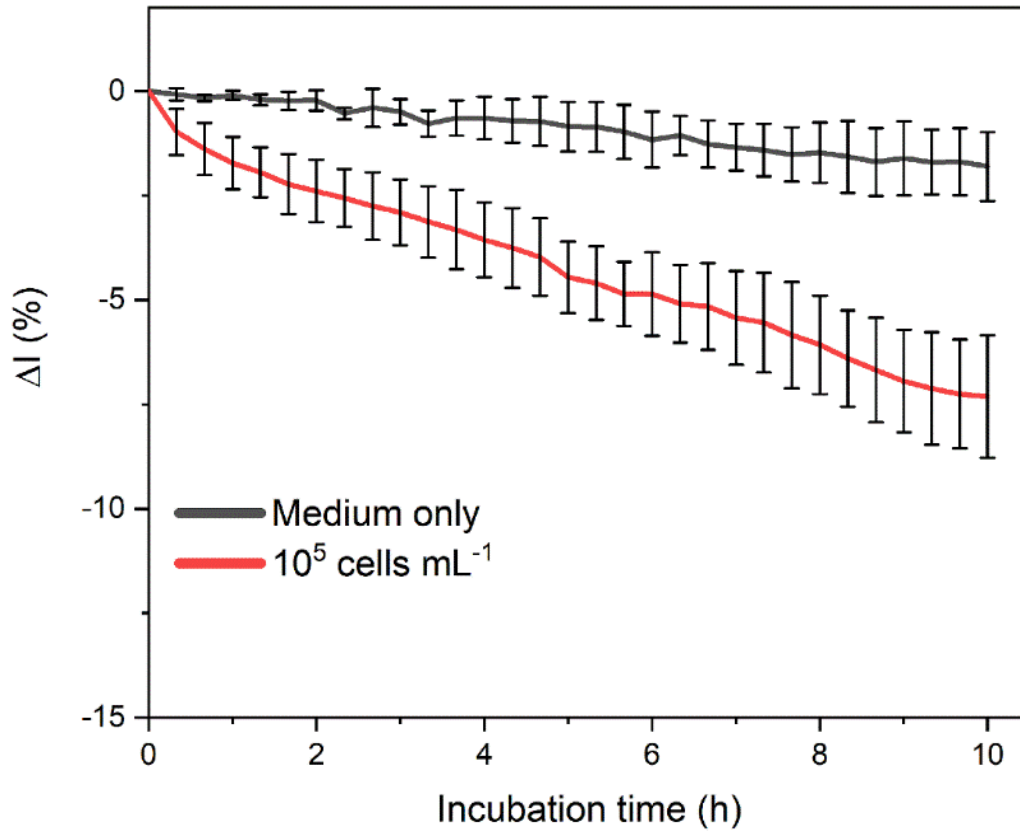
## Supporting Data

Figure S1A depicts a schematic illustration of the cross-section of the silicon microwell structure. The incident light is partially reflected from the bottom (orange arrow) and top (red arrow) interfaces of the silicon microwell grating, and the resulting reflectance spectra of the zero-order diffraction exhibit characteristic interference fringes (Figure S1B). The interference spectra are transformed into the corresponding single peaks by frequency analysis, allowing the monitoring of the reflected light intensity and the  $2nL$  value, as explained in the main article (Figure 1).



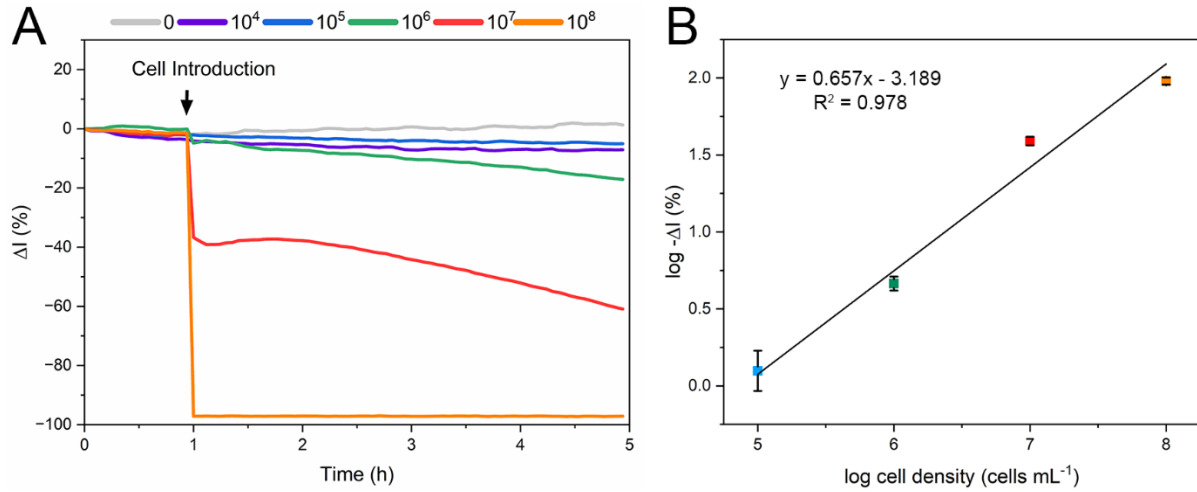
**Figure S1.** Microstructure and reflectance spectrum obtained from a photonic silicon chip. (A) Schematic illustration of the photonic silicon microwell gratings.  $L$  represents the height of the microstructure, and  $d$  is its width. Incident light hits both the bottom (orange arrow) and the top (red arrows) of the structure and is reflected from both interfaces. (B) The reflected light interferes, and the resulting reflectance spectra show characteristic interference fringes.

iPRISM for antifungal susceptibility testing (AFST) of *C. auris* was performed with cell suspensions at McFarland 2.0 ( $\sim 10^7$  cells  $\text{mL}^{-1}$ ; see Figure 1). The latter cell density is routinely used for AFST of *Candida* species by commercially available automated systems such as the Vitek2<sup>4</sup> and also expedites growth detection as compared to lower cell densities used in gold standard BMD ( $\sim 10^5$  cells  $\text{mL}^{-1}$ ) procedures.<sup>3</sup> Figure S1 demonstrates that at  $10^5$  cells  $\text{mL}^{-1}$ , growth detection in the iPRISM assay is feasible, slope:  $-0.73 \Delta I (\%) \text{ h}^{-1}$ . Yet, growth detection is clearly expedited at McFarland 2.0 with a slope of  $-10.8 \Delta I (\%) \text{ h}^{-1}$  (Figure 1).



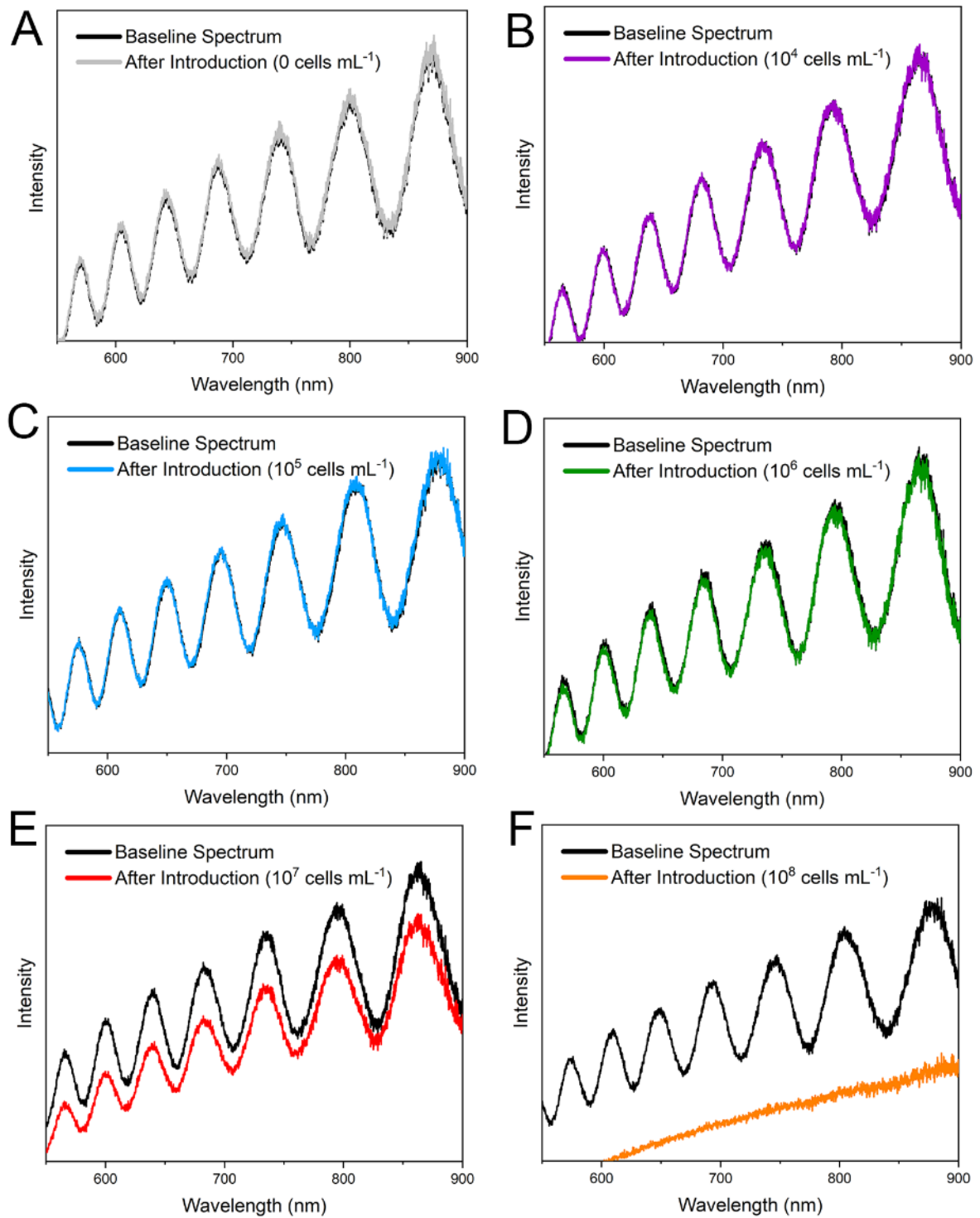
**Figure S2.** Averaged ( $n = 3$ ) iPRISM growth curves for *C. auris* at an initial cell density of  $10^5$  cells  $\text{mL}^{-1}$  and medium only. Error bars show standard deviations of these triplicate measurements.

Figure S3 shows the intensity change caused by the introduction of *C. auris* suspensions of different cell densities. Figure S3A depicts characteristic iPRISM curves, where the change in intensity  $\Delta I$  (%) is plotted over time, following the introduction of *C. auris* suspensions of different cell densities, and Figure S3B summarizes the respective average  $-\Delta I$  (%) in a log-log scale at a concentration range from  $10^5 - 10^8$  cells  $\text{mL}^{-1}$ . The decrease in light intensity is ascribed to light scattering induced by microbial cells, as described previously.<sup>5</sup>



**Figure S3.** Intensity changes after the introduction of *C. auris* suspensions of different cell density values compared to the baseline values plotted over time. (B) A calibration curve (log-log scale) showing the average  $-\Delta I$  (%) changes caused by the introduction of different *C. auris* cell concentrations ( $n = 3$ ). Error bars show standard deviation.

Figure S4 presents the raw reflectance spectra before and after the introduction of a concentration range from  $10^4$  –  $10^8$  cell  $\text{mL}^{-1}$ .



**Figure S4.** Change of the reflectance spectra after introduction of *C. auris* suspensions of different cell density values.

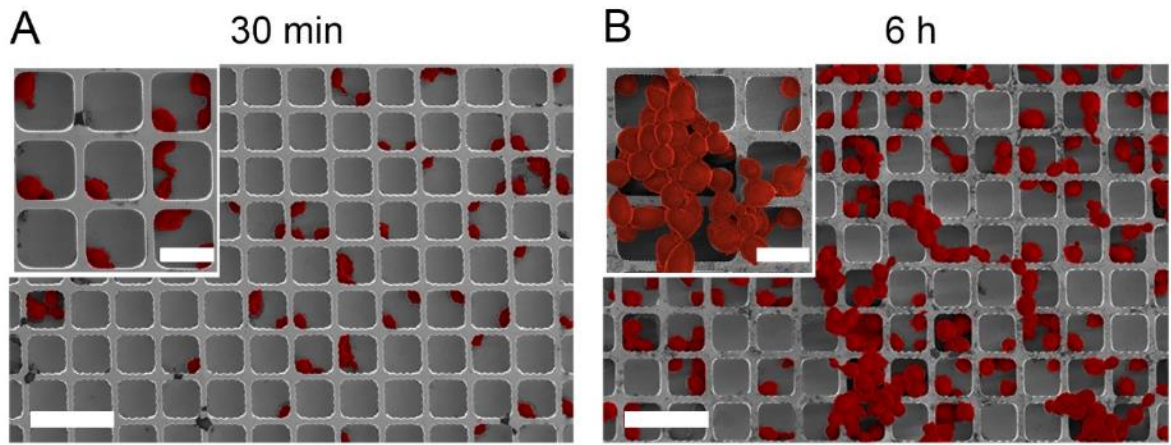


**Figure S5.** Scanning electron micrographs of *C. auris* (inoculum: McFarland 2.0) growing on the photonic silicon chips for (A) 30 min and (B) 6h, respectively. Scale bars correspond to 10  $\mu\text{m}$  and 4  $\mu\text{m}$  (inserts). Yeast cells were false-coloured in red for clarity.

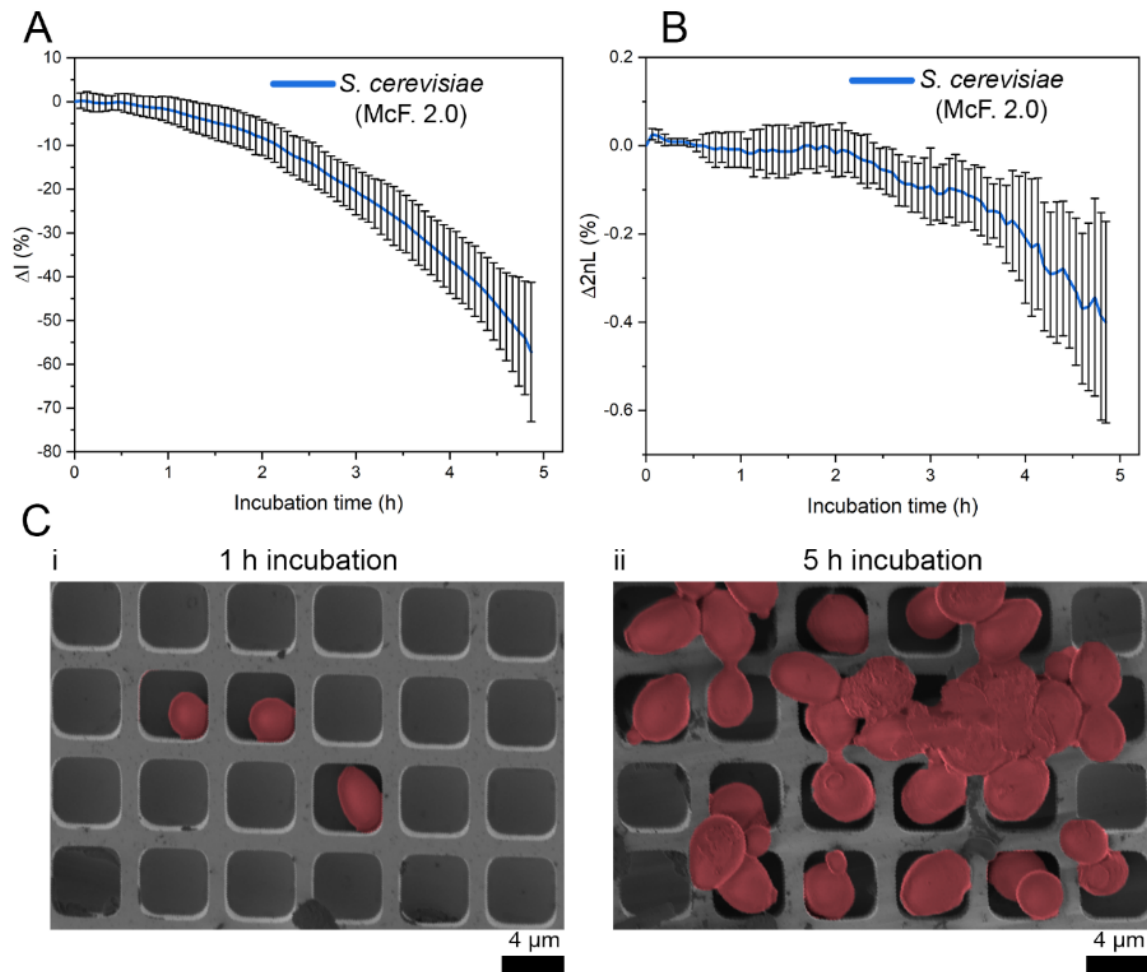


**Figure S6.** Averaged *S. cerevisiae* (i)PRISM growth curves ( $n = 3$ ) for (A) intensity (slope:  $-11.4 \Delta I (\%) h^{-1}$ ) and (B) 2nL (slope:  $-0.08 \Delta 2nL (\%) h^{-1}$ ) changes. The error bars show the standard deviation of the triplicate measurements. (C) Corresponding scanning electron micrographs after (C-i) 1h and (C-ii) 5 h of incubation. The yeast cells were false-coloured in red for clarity.



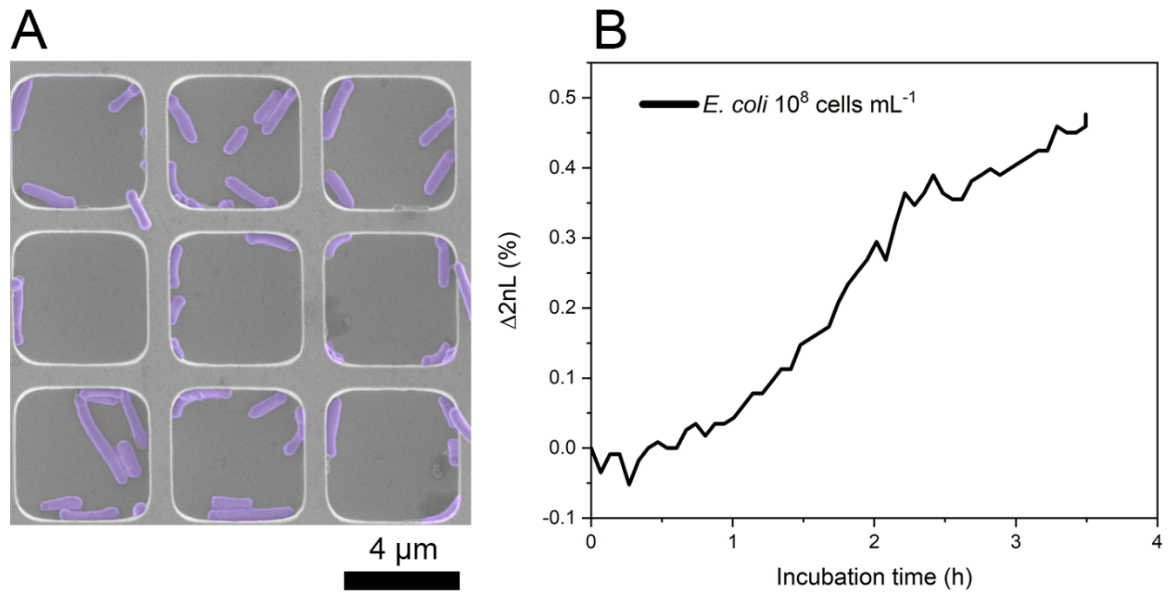


**Figure S7.** The bacterial species *E. coli* on photonic Si microwell chips. (A) A scanning electron micrograph demonstrates that most *E. coli* cells with a typical length of 1 – 2 μm reside within the microwell structure. The cells were false-coloured for clarity. (B) Bacterial proliferation within the microwells typically results in a 2nL increase ascribed to the increased refractive index within the microstructure due to bacterial growth.

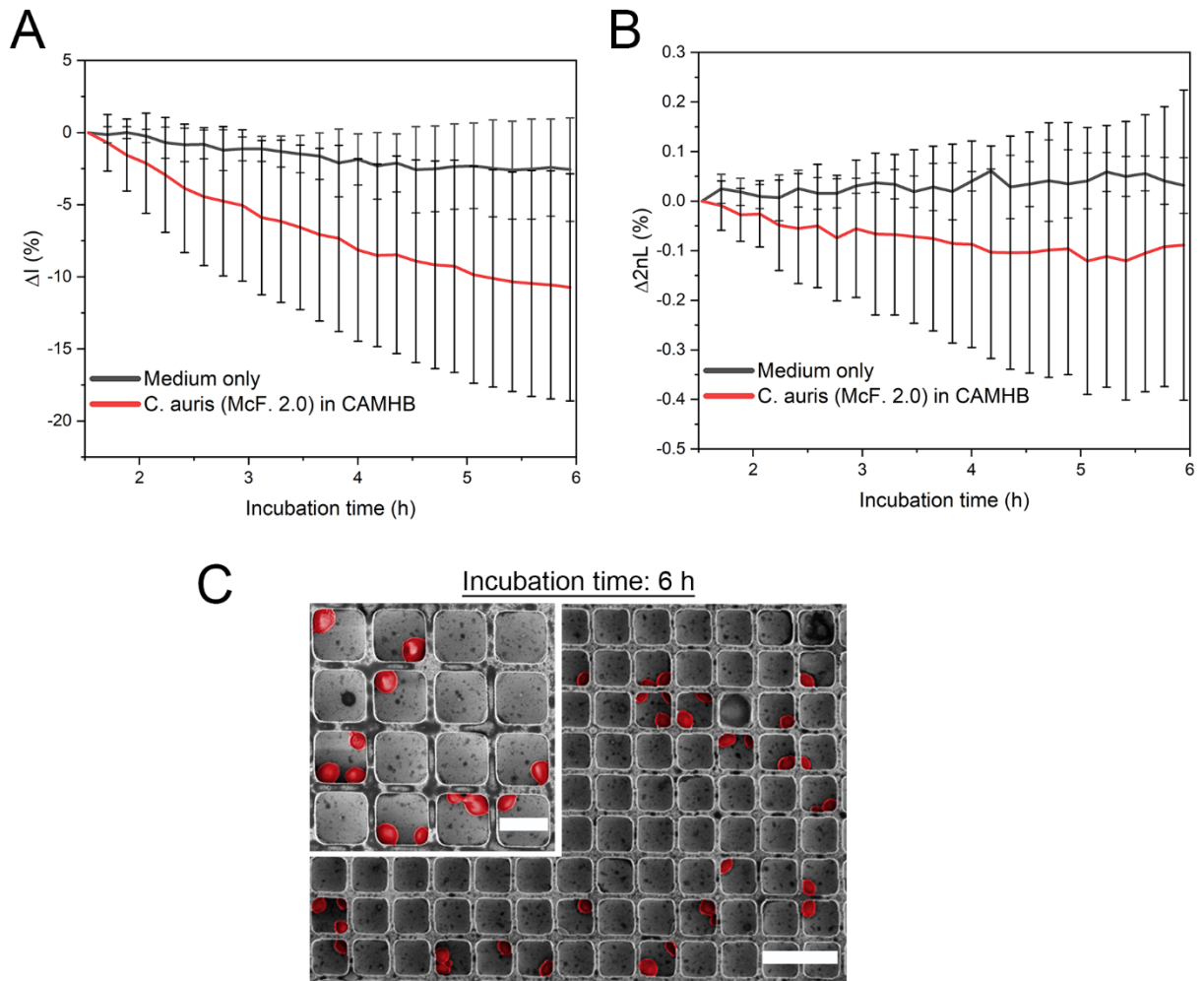


**Figure S8.** *C. auris* growing in cation-adjusted Muller Hinton Broth (CAMHB), a medium designated for antimicrobial susceptibility testing of bacteria. Averaged (i)PRISM growth curves for (A) intensity (slope:  $-1.8 \Delta I$  (%)  $h^{-1}$ ) and (B) 2nL (slope:  $-0.015 \Delta 2nL$  (%)  $h^{-1}$ ) signals of *C. auris* growing in CAMHB ( $n > 10$ ) and growth medium only as control ( $n = 3$ ). Error bars depict standard deviation. (C) Scanning electron micrographs after 6 h of incubation. The scale bars correspond to 10  $\mu m$  and 4  $\mu m$  (insert). Cells are false-coloured in red for clarity.

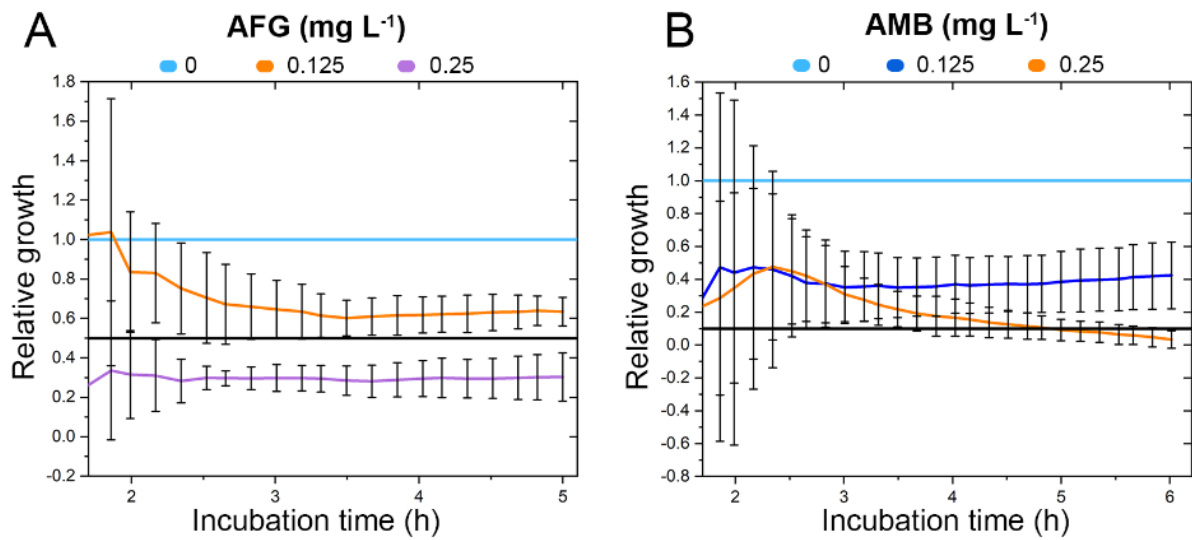


**Figure S9.** Relative growth was determined by iPRISM for the MIC, and the highest subinhibitory concentration for (A) anidulafungin (AFG) and (B) amphotericin B (AMB) against *C. auris* ( $n = 3$ ); error bars indicate standard deviations. The MIC can be determined within 3.5 h for anidulafungin and 6 h for amphotericin B as at these time points, the growth at the MIC and the highest subinhibitory concentration are significantly different (two-tailed t-test;  $p < 0.05$ ). Also, here all MIC growth curves fall below the MIC threshold (black lines) of 50 % (0.5) growth (anidulafungin) and 10 % (0.1) growth (amphotericin B).

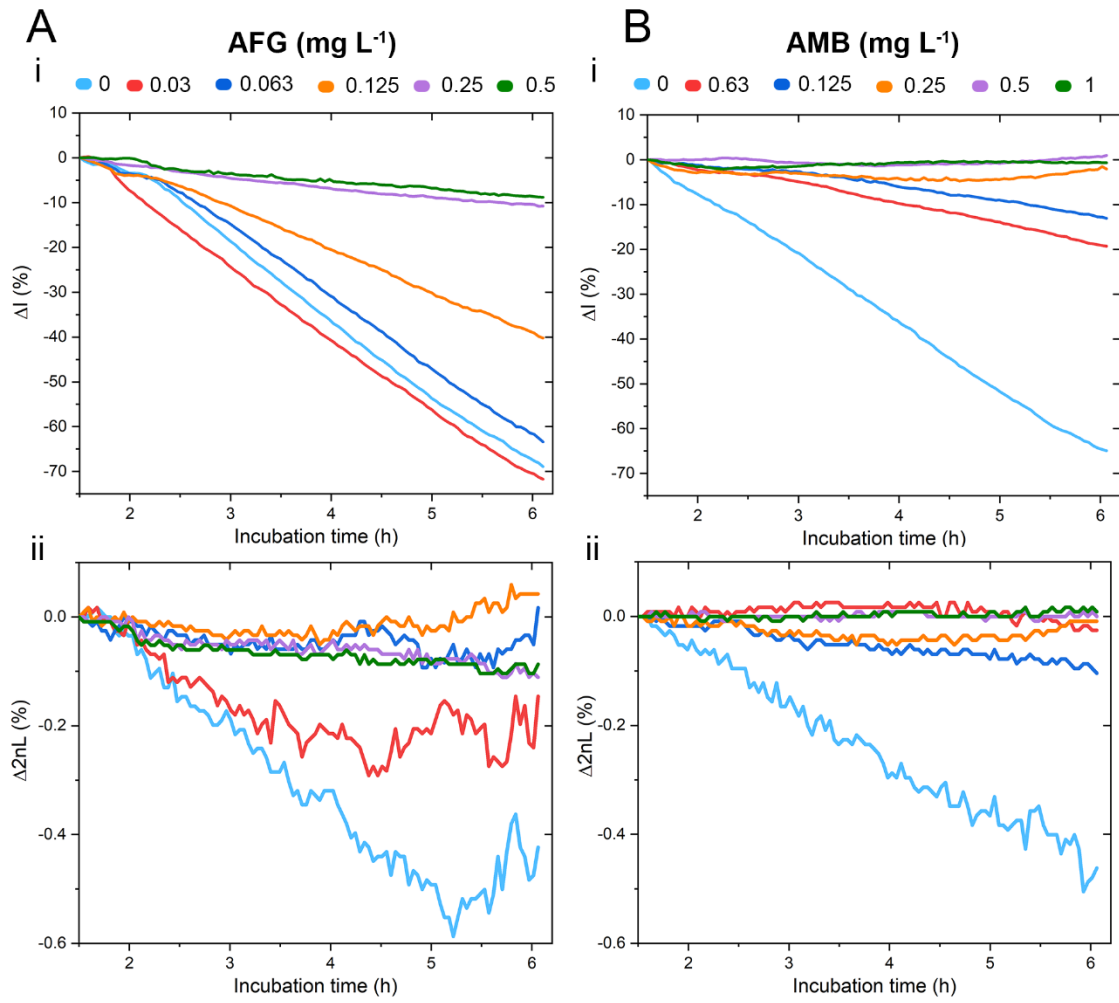


**Figure S10.** Growth curves for *C. auris* at varying antifungal concentrations by monitoring intensity and 2nL changes. (A-i) Intensity and (A-ii) 2nL changes for *C. auris* growing at varying anidulafungin concentrations. (B-i) Intensity and (B-ii) 2nL changes for *C. auris* exposed to different amphotericin B concentrations.

Figure S11 shows the growth curves obtained by a standard BMD assay for *C. auris* and amphotericin B, continuously monitored using a microplate reader. The MIC is determined to be 0.25 mg L<sup>-1</sup> as this concentration causes a > 90 % growth inhibition compared to the untreated no-drug control. The MIC (0.25 mg L<sup>-1</sup>) and the lowest subinhibitory concentration (0.125 mg L<sup>-1</sup>) are statistically different after 19 h (two-tailed t-test,  $p < 0.05$ ). Thus, the MIC can be determined within 19 h - an assay time which is still significantly longer than for the iPRISM assay (MIC determination within 6 h).

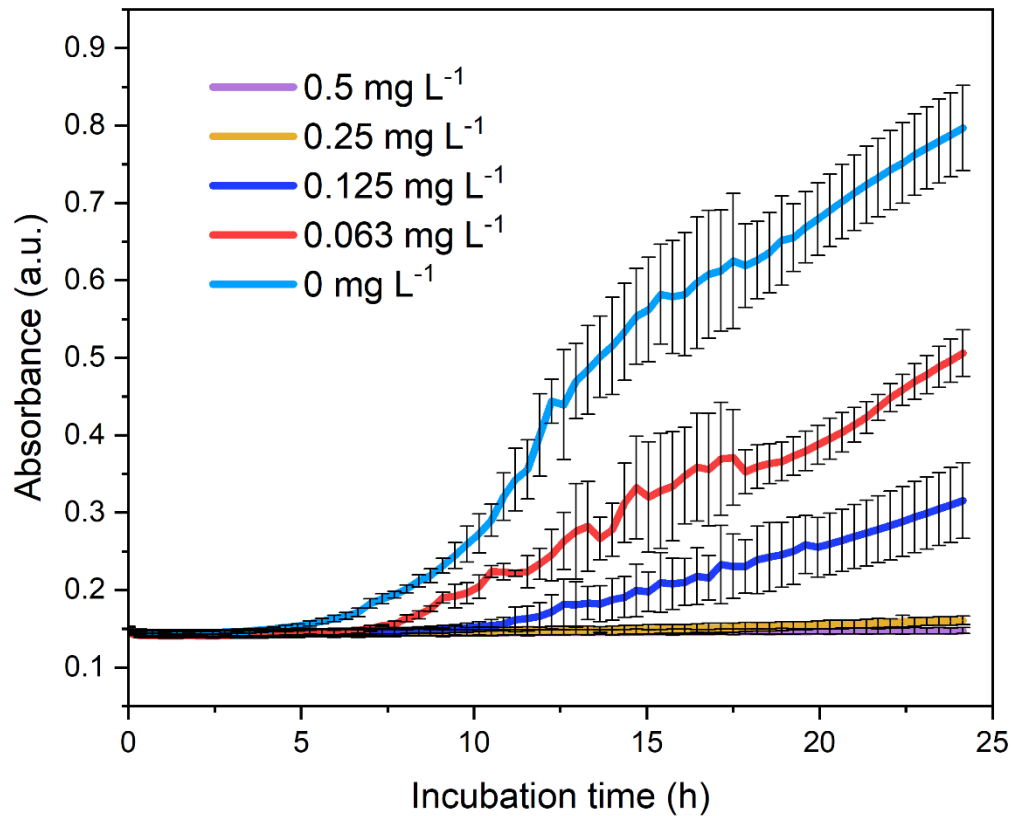


**Figure S11.** Continuous microplate reader measurements ( $n = 3$ ) for a standard BMD with *C. auris* and different amphotericin B concentrations over an incubation time of 24 h. Error bars indicate the standard deviation of the triplicate measurements.

**Table S1.** MIC value comparison for anidulafungin (AFG) and amphotericin B (AMB) obtained by iPRISM and gold standard BMD methods, including respective tentative epidemiological cut-off values (ECOFFs).

Antifungal	iPRISM		BMD		ECOFFs (mg L <sup>-1</sup> )
	MIC (mg L <sup>-1</sup> )	Time (h)	MIC (mg L <sup>-1</sup> )	Time (h)	
AFG	0.25	3.5	0.0625 mg L <sup>-1</sup>	24	0.25 - 2 <sup>6</sup>
AMB	0.25	6	0.125 - 0.25 mg L <sup>-1</sup>	24	1 - 2 <sup>6</sup>

## References

- 1 C. Heuer, J.-A. Preuss, M. Buttkewitz, T. Scheper, E. Segal and J. Bahnemann, *Lab Chip*, 2022, **22**, 4950–4961.
- 2 H. Leonard, S. Halachmi, N. Ben-Dov, O. Nativ and E. Segal, *ACS Nano*, 2017, **11**, 6167–6177.
- 3 EUCAST DEFINITIVE DOCUMENT E.DEF 7.3.2 Method for the determination of broth dilution minimum inhibitory concentrations of antifungal agents for yeasts, [https://www.eucast.org/fileadmin/src/media/PDFs/EUCAST\\_files/AFST/Files/EUCAST\\_E\\_Def\\_7.3.2\\_Yeast\\_testing\\_definitive\\_revised\\_2020.pdf](https://www.eucast.org/fileadmin/src/media/PDFs/EUCAST_files/AFST/Files/EUCAST_E_Def_7.3.2_Yeast_testing_definitive_revised_2020.pdf), (accessed March 2023).
- 4 E. Borghi, R. Iatta, R. Sciota, C. Biassoni, T. Cuna, M. T. Montagna and G. Morace, *J. Clin. Microbiol.*, 2010, **48**, 3153–3157.
- 5 N. Massad-Ivanir, Y. Mirsky, A. Nahor, E. Edrei, L. M. Bonanno-Young, N. Ben Dov, A. Sa'arb and E. Segal, *Analyst*, 2014, **139**, 3885-3894.
- 6 M. C. Arendrup, A. Prakash, J. Meletiadiis, C. Sharma and A. Chowdhary, *Antimicrob. Agents Chemother.*, 2017, **61**.